Physica E 42 (2010) 2295–2300

Contents lists available at ScienceDirect

Physica E

journal homepage: www.elsevier.com/locate/physe

Sliding oscillation of multiwall carbon nanotubes

R. Chowdhury, C.Y. Wang*, S. Adhikari, F.M. Tong

School of Engineering, University of Swansea, Singleton Park, Swansea, Wales SA2 8PP, UK

ARTICLE INFO

Article history:
Received 7 March 2010
Received in revised form
8 May 2010
Accepted 10 May 2010
Available online 13 May 2010

Keywords:
Multiwall carbon nanotubes
Sliding oscillation
Finite element method

ABSTRACT

The sliding oscillations of multiwall carbon nanotubes (MWCNTs) with open ends are characterized. The interlayer van der Waals interaction provides a restoring force for the oscillatory system whereas the ultralow interlayer friction was ignored due to its negligible influence on the oscillation. Based on this model, various oscillation modes were obtained with the associated frequency of the order 1–100 GHz by using the finite element method. The radius and length dependence and the effect of end constraints have been further studied and quantified for the sliding oscillation of MWCNTs. The results are interpreted in terms of the mass change and the restriction on the motion of the individual tubes of MWCNTs. In view of these analyses, MWCNTs with open ends may expect to serve as nanoscale oscillatory devices where the oscillation modes and frequency can be controlled by choosing the tube geometry and imposing desirable end constraints.

1. Introduction

Vibration of carbon nanotubes (CNTs) has been studied extensively in the last two decades [1]. It was shown [2,3] that these nanotubules can be terahertz nanoresonators which are promising for nanoscale sensors, transducers and actuators [4]. In the vibration analyses of CNTs special attention was paid to the radial breathing vibration [5–7], beam-like bending vibration [8–12] and axisymmetric axial vibration [10–13], which serve as useful probes for the geometric size, atomic structures and elastic properties of CNTs and thus are of major scientific and engineering interest. In 2000, Cumings and Zettl [14] experimentally observed sliding motion of a multiwall CNT (MWCNT) where the inner tubes slide relative to the outermost tube with open ends. The observation demonstrated that such an MWCNT system has the potential to be low wear nanobearings, nanosprings and nanooscillators that form essential components of Nano-Electro-Mechanical systems. Such a sliding motion of the adjacent layers also offers a good testing platform for the study of the interlayer interaction of MWCNTs including the interlayer friction and interlayer van der Waals (vdW) interaction. The sliding behaviors of MWCNTs thus have attracted considerable attention in nanomechanics community [14–24].

In 2002, motivated by Cumings and Zettl's work, Zheng and Jiang [15] developed a continuum model based on Lennard-Jones potential [25] to account for the sliding oscillation of double wall CNTs (DWCNTs) in terms of the interlayer van der Waals (vdW) interaction. The predicted frequency of the DWCNT oscillator is of the order 0.1–1 GHz. In addition, consistent with the experimental observation [14], the authors showed that the interlayer friction of DWCNTs is ultralow and cannot significantly affect the oscillation frequency. One year later Rivera et al. [16] conducted molecule dynamics (MD) simulations on a similar oscillatory system of DWCNTs. The results showed again that a DWCNT could be a gigahertz oscillator when the inner tube was pulled out and then released. However, such an oscillation was damped by the interlayer friction arising from the thermal fluctuation in the conformation of the DWCNT. Interestingly, both experimental and theoretical studies [14–16] indicated that the interlayer vdW interaction offered a constant restoring force for the MWCNT oscillatory system, which is independent of the relative displacement between adjacent layers. These early studies [14–16] stimulated a significant wave of exploration on the oscillatory sliding of MWCNTs in recent research [18–24]. The studies were largely focused on the unique features of the nanoscale friction between the adjacent layers of MWCNTs. The oscillation velocity [18,24], the end conditions [18], defects [23] of individual tubes and the commensuration between the adjacent tubes [20,22] of MWCNTs are identified as the possible origins of the interlayer friction. On the other hand, detailed studies on the sliding oscillation of MWCNTs themselves have not been available in the literature due to lack of an efficient model for MWCNTs as oscillatory systems.

In the present study we shall conduct a comprehensive investigation on the sliding vibration of MWCNTs to quantify the oscillatory frequency, predict the associated oscillatory mode and examine the effect of dimensional factors and end constraints on the sliding oscillation of MWCNTs. A finite element method

* Corresponding author.
E-mail address: Chengyuan.wang@swansea.ac.uk (C.Y. Wang).

1386-9477/$ - see front matter © 2010 Elsevier B.V. All rights reserved.
doi:10.1016/j.physe.2010.05.003

(FEM) validated and first used in the buckling analysis of MWCNTs [26] will be further extended to the oscillation analysis of MWCNTs. The emphasis will be placed on novel physical phenomena arising from the coupled multilayer structure of CNTs. It is expected that the present work will bring in better understanding of the nanostructures of MWCNTs and provide a comprehensive guidance for the conceptual design of CNT-based nanooscillators in future nanotechnology.

2. Modeling and method of analysis

The finite element (FE) model for MWCNTs is generally developed based on the modeling criteria determined by Wang et al. [27]. In this model the constituent tubes of MWCNTs were modeled by adopting solid shell elements. The mesh designs were kept consistent for all analyses such that each tube consists of 36 elements in the circumferential cross sectional plane and $(45L/10R)$ elements in the longitudinal direction. Here L is the length and R is the mid-surface radius of the tube. The vdW interactions between adjacent tubes were simulated by linear spring elements which are represented by lines in Fig. 1 for a double wall CNT. The stiffness k of the spring is given by

$$k=\frac{c}{2}(A_i+A_o) \tag{1}$$

and the interlayer vdW interaction coefficient c is estimated as $c=102$ GPa/nm [10,11,28]. Here A_i and A_o denote the mid-areas of the inner and outer shell elements, respectively, which can be calculated by $A_i=2\pi R_i L$ and $A_o=2\pi R_o L$, where, as shown in Fig. 1, R_i and R_o denote the mid-surface radii of the inner and outer cylindrical shell elements, respectively. The potential energy $U(s,x)$ of the interlayer vdW interaction modeled by the spring system is a function of the interlayer spacing s and the axial distance x between the centers of two adjacent layers. The vdW radial pressure is calculated by $\partial U(s,x)/\partial s$ while the vdW axial stress is given by $\partial U(s,x)/\partial x$. On the other hand, the low interlayer friction cannot significantly change the oscillation frequency of MWCNTs [14,15,23] and thus is neglected in the present study.

The method to impose the boundary conditions in this study was similar to that of Refs. [26,28] whereby two types of end constraints are considered for the constituent tubes of MWCNTs, i.e., simply supported (SS) end with $v=0$, $w=0$ and $\partial^2 w/\partial x^2=0$ and clamped (C) end with $u=0$, $v=0$, $w=0$ and $\partial w/\partial x=0$. Here u, v and w denote the displacements of the ends in the longitudinal, circumferential and radial directions, respectively. The reader may refer to Refs. [26–28] for further discussions on the modeling methodology used in the present study. Note that half (symmetry) models were used to reduce computational time and also allow for the deformation of the inner tube to be graphically viewed. The oscillation analysis of the MWCNTs was carried out using the ANSYS FE software package. Here it should be pointed out that the finite element shell model is not capable of treating nanotube chirality. However, since the tube chirality is expected to have negligible effect on the vibration of CNTs, this limitation cannot lead to significant errors in our results. Indeed, in our previous work the present model was efficiently applied to the buckling and vibration analyses of MWCNTs [26,28], where the buckling results given by the present model are found to be in good agreement with those given by other models [26]. In particular, as will be shown later (Section 3.2), the diameter and radius dependence of sliding oscillation predicted based on the present FE model is in qualitative agreement with the dependence predicted by multi-scale simulations in Refs. [15,16]. However, the quantitative comparison of the present model with other models is not yet available due to lack of data for the sliding oscillation of MWCNTs.

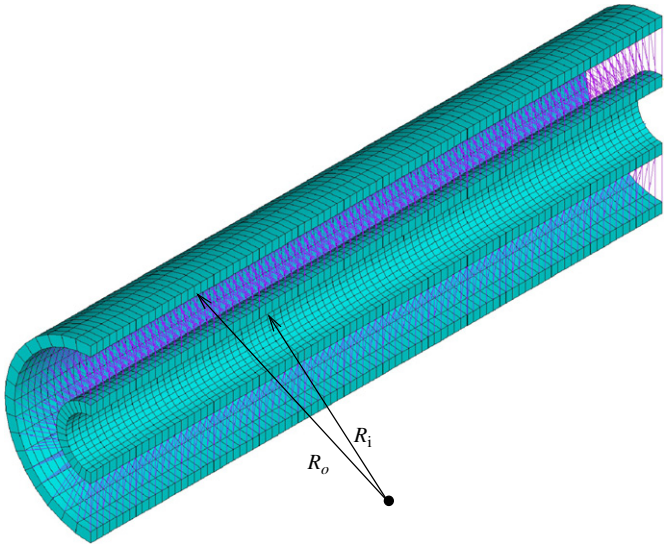

Fig. 1. The finite element model of a double wall CNT. The figure shows the discretisation of the inner and the outer tube with mid-surface radii R_i and R_o, respectively. Mid-areas A_i and A_o can be calculated from mid-surface radii R_i and R_o, respectively. The linear springs representing the vdW interaction are shown by lines.

3. Results and discussion

In this section, the above ANSYS model will be employed to study the sliding oscillation of MWCNTs. Five-wall CNTs in Table 1 are chosen as typical examples, which can be classified into six categories, i.e., (1) thin (Example 1), (2) thick (Example 2), (3) almost solid (Example 3) MWCNTs with the innermost radius-to-thickness ratio R_i/H decreasing from 5, 1 to 0.25, (4) short (Example 3), (5) intermediate (Example 4) and (6) long (Example 5) MWCNTs with the length-to-the outermost diameter aspect ratio L/D_0 increasing from 5, 10 to 20. Both simply supported and clamped ends are considered for individual tubes of these examples. The values of equivalent material and geometric constants of single wall CNTs (SWCNTs) used in the present study are Young's modulus $E=3.5$ TPa, the effective wall thickness $h=0.1$ nm [30], Poisson's ratio $v=0.2$ [31,32] and the mass density per unit volume $\rho=2.27$ g/cm^3 [29].

3.1. Sliding oscillation of MWCNTs

In what follows, we study the sliding oscillation of MWCNTs where the two ends of each constituent tube are open and simply supported. To this end the first five vibration modes given by the ANSYS model are shown in Fig. 1 for the five examples in Table 1.

Table 1
Five-wall CNTs as typical examples of MWCNTs considered in the present study.

	Examples				
	1 Thin	2 Thick	3 Solid/short	4 Solid/intermediate	5 Solid/long
R_i (nm)	6.8	1.36	0.34	0.34	0.34
H (nm)	1.36	1.36	1.36	1.36	1.36
L (nm)	81.6	27.2	17	34	68
$L/(D_0)$	5	5	5	10	20
R_i/H	5	1	0.25	0.25	0.25

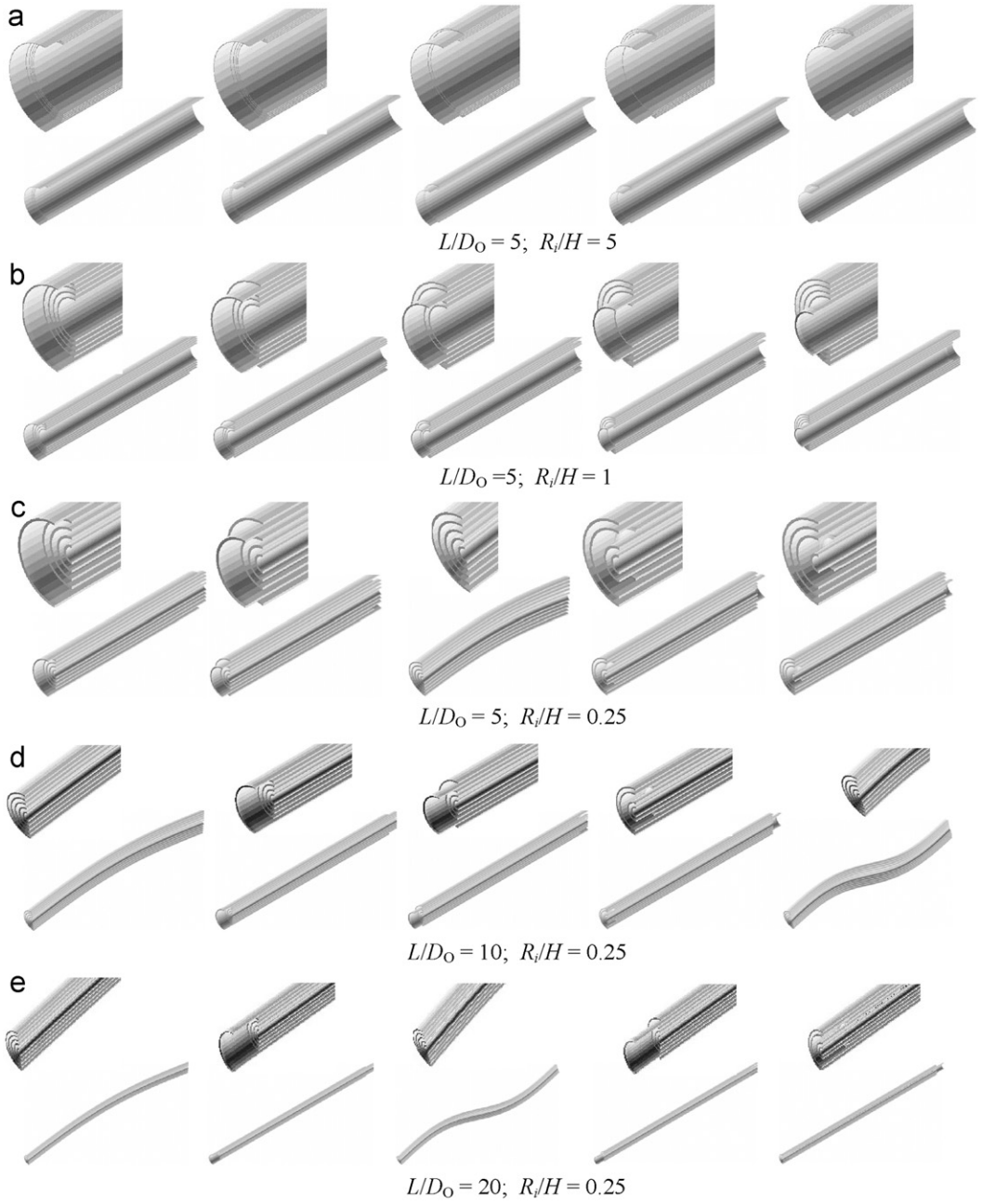

Fig. 2. First five vibration modes of 5-wall CNT with SS–SS boundary condition: (a) Example 1; (b) Example 2; (c) Example 3; (d) Example 4; (e) Example 5. The edge of the MWCNT is zoomed to show the sliding mode for clarity.

It can be seen from Fig. 2(a) and (b) that, in Examples 1 and 2 (with $L/D_0=5$ and $R_i/H=5$ and 1, respectively) the first vibration mode associated with fundamental frequency is characterized by the rigid body translation of the outermost layer with respect to the core layers in axial direction. A similar sliding oscillation of CNTs has also been observed in experiment [13] and multi-scale simulations [14,15]. In Fig. 2(a) and (b), when the mode number increases (i.e., the frequency rises) different sliding oscillations are achieved, where the oscillation of one individual tube relative to other layers is transferred sequentially from the outermost layer to the innermost layer. The sliding oscillations are also observed for Example 3, a (almost) solid MWCNT with $L/D_0=5$ and $R_i/H=0.25$, i.e., modes 1, 2, 4 and 5 in Fig. 2(c).

The frequencies of the vibration modes in Fig. 2 are shown graphically in Fig. 3 for Examples 1–3. As seen in Fig. 3 the oscillation frequencies of the three examples generally increase

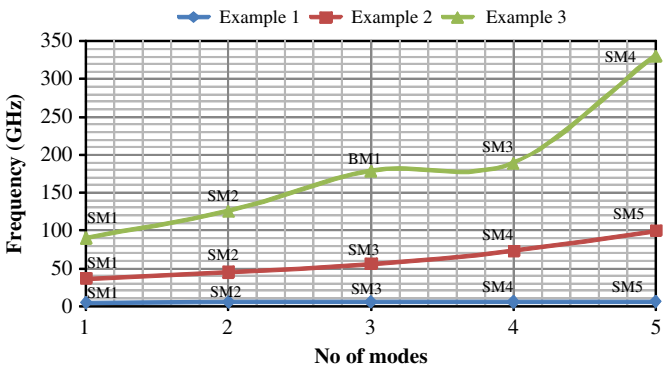

Fig. 3. Dependence of radius on vibration frequency of 5-wall CNT, for constant aspect ratio ($L/D_0=5$) with a different innermost radius. SM1, …, SM5 represent sliding modes. BM1, …, BM5 represent bending modes.

when the oscillating tube changes from the outermost layer, to the next layer and finally to the innermost one, which are denoted by SM1 (sliding mode), SM2, …, SM5, respectively. This tendency becomes more pronounced when the innermost radius of the MWCNTs decreases from 6.8 to 0.34 nm. For example, when the sliding modes change from SM1 of the outermost layer to SM5 of the innermost one the oscillation frequency of Example 1 almost remains unchanged at 4.3 GHz while that of Example 3 rises drastically from 90 GHz of SM1 to 330 GHz of SM4. In addition, contrary to the case of Examples 1 (a thin MWCNT) and 2 (a thick MWCNT), where the first five modes are all sliding oscillations (Fig. 2(a) and (b)), transverse bending vibration ($f_3=177.68$ GHz) is observed for Example 3 as the third mode (Fig. 2(c)) where the half axial wave number is one. As shown in Fig. 3, for Example 3 the energy of the sliding oscillations SM3 and SM4 of tubes 3 and 4 (tube 1 is the outermost layer), respectively, is even higher than that of the aforementioned bending vibration detonated as BM1. Further increasing the aspect ratio of Example 3 from 5 to 10 and to 20 we obtain Examples 4 and 5 of Table 1, which are considered as intermediate and long MWCNTs, respectively. In this case the constituent tubes have a large aspect ratio ranging from 10 to 100, i.e., they have typical beam-type structures. As can be observed in Fig. 2(d) and (e), the fundamental frequency of these two examples always corresponds to the first transverse bending mode (BM1). The second bending mode (BM2) is identified as modes 5 and 3 for Examples 4 and 5, respectively, while other three modes in Fig. 2(d) and (e) are the sliding oscillation similar to those of Examples 1–3. The frequencies of these modes are plotted in Fig. 4 for Examples 4 and 5. It is noted that the transverse bending vibration of MWCNTs is characterized by a circular cross-section and almost unchanged interlayer spacing [10,11]. Naturally the frequency or energy of such a bending mode is determined primarily by the flexural rigidity of MWCNTs as equivalent nano-beams. In contrast, the sliding oscillation of MWCNTs is mainly controlled by the interlayer vdW interaction instead of material or structural properties of CNTs. The above observation suggests that when the aspect ratio of MWCNTs is sufficiently large, say larger than 10, the interlayer vdW interaction could exert comparable or even stronger effects on their mechanical behaviors than the flexural rigidity of MWCNTs.

3.2. Effect of geometrical size

It was shown in the preceding section that the oscillatory behavior of MWCNTs will change significantly with their geometrical size, such as the radius and length of the oscillating tubes. Next we examine this issue in detail.

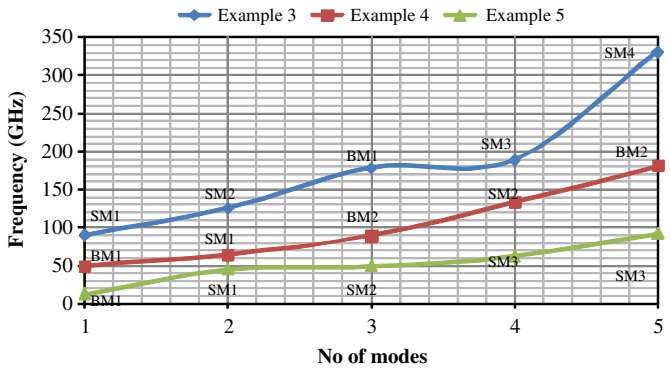

Fig. 4. Dependence of aspect ratio on vibration frequency of 5-wall CNT, for constant innermost radius ($R_i/H=0.25$) with a different aspect ratio. SM1, …, SM5 represent sliding modes. BM1, …, BM5 represent bending modes.

First we study the dependence of the sliding oscillation on the (innermost) radius of MWCNTs. To this end we consider Examples 1–3 of Table 1 with the innermost radius decreasing from 6.8 to 0.34 nm and constant aspect ratio 5. It is seen in Fig. 3 that the frequency of the sliding modes increases considerably when the innermost radius decreases. In particular, when the sliding oscillation changes from SM1 of the outermost layer, to SM2 of the adjacent layer and finally to SM5 of the innermost layer the associated frequency turns out to be more and more sensitive to the decreasing innermost radius. Indeed, as the innermost radius reduces from 6.8 nm of Example 1 to 0.34 nm of Example 3, the frequency of SM1 upshifts from 4.26 to 90 GHz, while that of SM4 is raised substantially from 5.59 to 330 GHz. The dependence of the sliding oscillation on the length of MWCNTs can be clearly seen in Fig. 4 obtained for Examples 3–5, where the length of MWCNTs increases from 17 to 68 nm while the innermost radius remains unchanged at 0.34 nm. As shown in the figure, the frequencies of sliding modes SM1, SM2 and SM3 decrease considerably with the increasing length of the five-wall CNTs. For instance, as the length becomes four times as much as its original value of 17 nm the frequency of all sliding modes decreases approximately by a factor of two.

It is noted that such a radius and length dependence obtained based on the present ANSYS model is in qualitative agreement with the prediction given by previous multi-scale simulations [15,16]. The numerical results can be explained by the unique features of an MWCNT oscillatory system demonstrated in Refs. [14–16]. In these studies the authors revealed that the restoring force of the oscillation of individual tubes is determined by the rate of change of the interlayer (vdW interaction) potential relative to the extrusion of the oscillating tube and thus is independent of the length of the MWCNT. In addition, the radius dependence of the interlayer vdW interaction, which is weak especially for the tubes of large radius, say >2 nm [15], has been neglected in the present study. It follows that reducing the innermost radius and length of the MWCNT does not significantly affect the restoring force of the system but leads to decreasing mass of all the oscillating tubes, which therefore upshifts the frequency of all sliding modes of the MWCNT. Similar theory can also be used to elucidate the increase of the sliding frequency obtained in Fig. 3 when the oscillation modes change from SM1 of the outermost tube with the largest radius to SM5 of the innermost one with the smallest radius.

3.3. Boundary condition effect

In this section we examine the effect of end constraints on the sliding oscillation of MWCNTs. In doing this, we sequentially clamp one end of the constituent tubes of originally simply supported MWCNTs until all the constituent tubes are clamped at one end while the other end is still simply supported. This clamping procedure is carried out in the following sequences: clamp the outermost tube first, then its adjacent tube, and finally the innermost tube. The dependence of frequencies and mode shapes on the number of clamped tubes N is calculated and plotted in Fig. 4 for Example 1. As seen in Section 3.1, Example 1 consists of short constituent tubes with a small aspect ratio 5. When the tube is simply supported it exhibits sliding oscillation associated with the five lowest frequencies. In Fig. 5(a) we found that clamping the outermost tube prohibits SM1 of Example 1. This is simply because the clamped outermost layer cannot move in axial direction. In this case, the fundamental frequency is associated with SM2 of the second layer and the following three modes with higher frequencies are SM3, SM4 and SM5 of the next three inner layers, respectively. These are almost the same as those of the

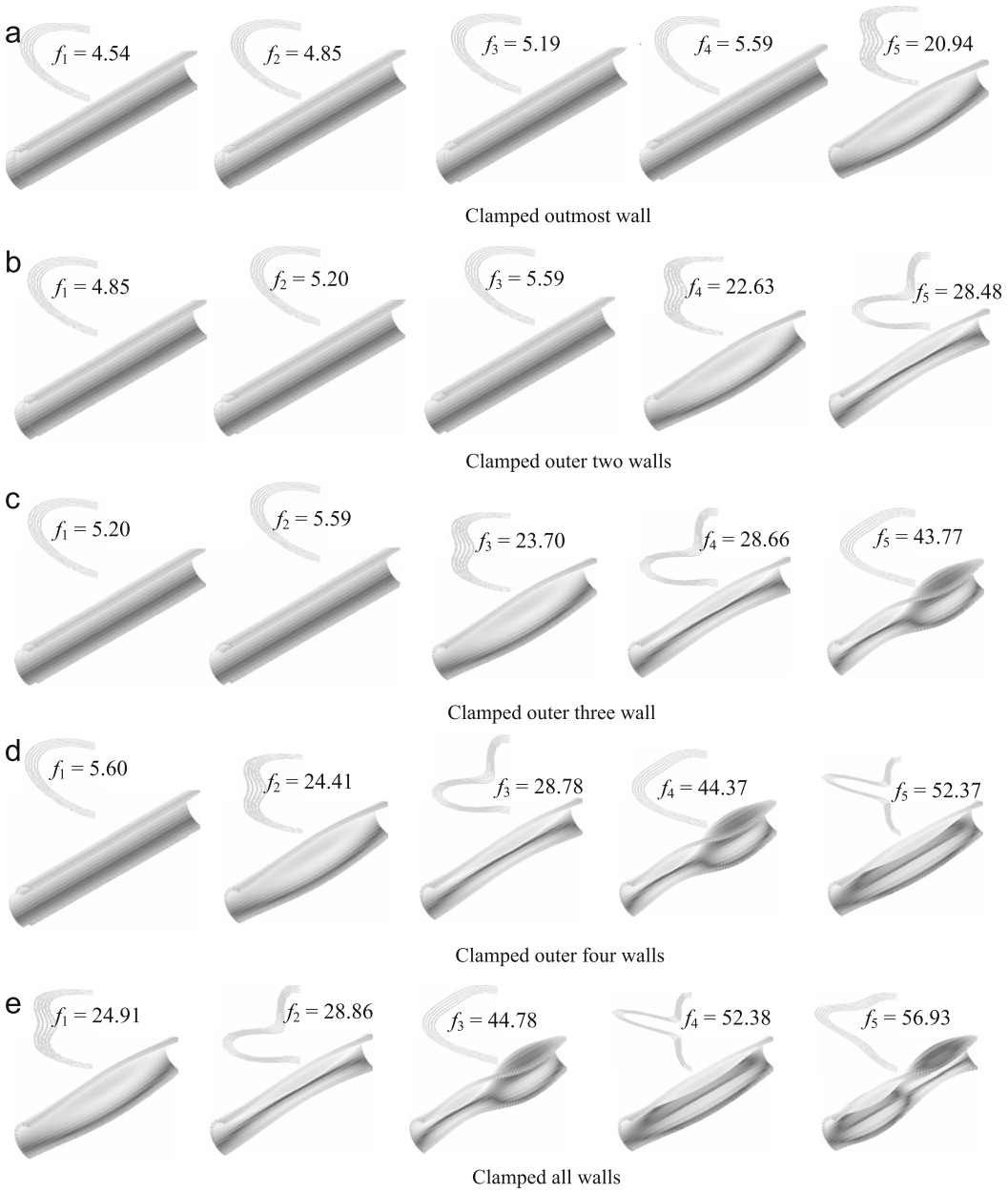

Fig. 5. First five vibration modes of 5-wall originally SS–SS CNT (Example 1) with clamping at the end of the wall, sequentially from outermost wall to innermost wall. All the frequency values are in GHz units.

MWCNTs with two simply supported ends (SS–SS) except that the oscillation frequencies of SM2–SM5 are about 6% higher than those of the SS-SS case. To get some idea, clamping the outermost layer will slightly upshift the frequency of SM2 from 4.26 to 4.54 GHz. It is also shown in Fig. 5(a) that at the highest frequency considered here (mode 5), the system exhibits circumferential mode where the walls of constituent tubes are bent/stretched along circumferential and longitudinal directions. Specifically, the frequency only rises marginally from 4.5 GHz of SM2 to 5.6 GHz of SM5 but it increases drastically to 21 GHz when the circumferential mode is achieved. Further increasing the number of clamped layers restricts the sliding oscillations of the inner tubes. As a result, more circumferential modes are found in the first five modes in Fig. 5(b) and (c). Naturally, clamping all the constituent tubes at one end completely eliminates the sliding oscillations of Example 1 and all five low frequency oscillations turn into the circumferential modes as shown in Fig. 5(e). As mentioned above the oscillating frequency of individual tubes rises significantly when the outermost layer of the simply supported MWCNT is fixed. However, as shown in Fig. 5, on further clamping the inner layers the oscillating frequencies obtained for the individual tubes remain almost unchanged, which are up to 10 times lower than those of circumferential modes. Since the frequency of circumferential modes is primarily determined by the wall rigidity of MWCNTs, e.g., bending rigidity and in-plane extension rigidity, the frequency of the circumferential modes basically measures the effects of the wall rigidities of CNTs, which can be regarded as material constants [30]. Thus, the much higher frequency of the circumferential modes indicates that for MWCNTs the wall rigidities play a more important role than the interlayer vdW interaction in determining the mechanical behavior of the MWCNT. In addition, it is seen that enforcing clamped end constraints on individual tubes enables us to intentionally choose oscillating tubes, i.e., the sliding modes, and also moderately adjust the frequency of particular sliding oscillation mode in the design of MWCNT-based nanoscale oscillatory systems.

4. Conclusions

We have investigated the axial oscillations of MWCNTs and their dependence on the geometric sizes and boundary conditions. The simply supported boundary conditions are applied to six types of MWCNTs as shown in Table 1, such as thin, thick and almost solid MWCNTs, and short, intermediate and long MWCNTs. The heterogeneous boundary conditions (i.e., some tubes of MWCNTs have two ends simply supported while other tubes have one end simply supported and the other fixed) are also considered for the oscillation of thin MWCNTs. The major conclusions arising from the present study are summarized as follows:

(1) MWCNTs with simply supported open ends can serve as nanoscale oscillators where one constituent tube slides back and forth in axial direction relative to others. For thick and solid MWCNTs the frequency of such oscillations increases rapidly when the oscillating tube changes from the outermost tube to the innermost one. However, in the case of thin MWCNTs the frequency remains almost constant. The frequency of axial oscillation ranges from the order of 1 to 100 GHz.
(2) The frequency of the axial oscillation increases substantially with decreasing radius and length of MWCNTs due to the declining mass of the oscillating tubes. Such radius and length dependence becomes more pronounced for the higher frequency oscillation of the inner tubes.
(3) Clamping the constituent tubes prevents the axial oscillation of the clamped tubes and tends to increase the oscillation frequency of other tubes. Specifically, clamping the outermost tube of simply supported MWCNTs will upshift the oscillation frequency of other tubes by around 6%. Such an effect however is negligible when the inner tubes are clamped.
(4) The comparison of frequency among axial oscillation, transverse bending and circumferential modes indicates that the wall stiffnesses of constituent tubes exert much stronger influence than the interlayer vdW interaction on the mechanical responses of MWCNTs whereas for slender MWCNTs, say length-to-diameter ratio larger than 10, the influence of the interlayer vdW interaction could be more significant than that of transverse bending stiffness of MWCNTs as nanoscale beams.

Nanometer-scale oscillators are promising for critical components of Nano-Electro-Mechanical systems (NEMS) such as actuators, charge detection devices and parametric amplifiers. Thus the results obtained in the present study are essential for the development and conceptual design of NEMS devices based on MWCNT oscillators.

References

[1] R.F. Gibson, E.O. Avorinde, Y.F. Wen, Compos. Sci. Technol. 67 (2007) 1.
[2] C.Y. Li, T.W. Chou, Phys. Rev. B 68 (2003) 073405.
[3] C.Y. Li, T.W. Chou, Appl. Phys. Lett. 84 (2004) 5246.
[4] P. Ball, Nature 414 (2001) 142.
[5] A.M. Rao, J. Chen, E. Richter, U. Schlecht, P.C. Elund, R.C. Haddon, U.D. Venkateswaran, Phys. Rev. Lett. 86 (2001) 3895.
[6] M.S. Strano, S.K. Doorn, E.H. Haroz, C. Kittrell, R.H. Hauge, R.E. Smalley, Nano Lett. 3 (2003) 1091.
[7] N. Izard, D. Riehl, E. Anglarget, Phys. Rev. B 71 (2005) 195417.
[8] R. Gao, Z.L. Wang, Z. Bai, W. de Heer, L. Dai, M. Gao, Phys. Rev. Lett. 85 (2000) 622.
[9] H. Jiang, M.F. Yu, B. Liu, Y. Huang, Phys. Rev. Lett. 93 (2003) 185501.
[10] C.Y. Wang, C.Q. Ru, A. Mioduchowski, Phys. Rev. B 72 (2005) 075414.
[11] C.Y. Wang, C.Q. Ru, A. Mioduchowski, J. Appl. Phys. 97 (2005) 114323.
[12] F. Scarpa, S. Adhikari, J. Non-Cryst. Solids 354 (2008) 4151.
[13] C.E. Bottaini, A. Li, M.G. Bassi, A. Podesta, P. Miani, A. Zakhidow, R. Baughman, D.A. Walter, R.E. Smalley, Phys. Rev. B 67 (2003) 155407.
[14] J. Cumings, A. Zettl, Science 289 (2000) 602.
[15] Q.S. Zheng, Q. Jiang, Phys. Rev. Lett. 88 (2002) 045503.
[16] J.L. Rivera, C. McCabe, P.T. Cummings, Nano Lett. 3 (2003) 1001.
[17] A.V. Belikov, Y.E. Lozovik, A.G. Nikolaev, A.M. Popov, Chem. Phys. Lett. 385 (2004) 72.
[18] P. Tangney, S.G. Louie, M.L. Cohen, Phys. Rev. Lett. 93 (2004) 065503.
[19] E. Bichoutskaia, E.A.M. Popov, A. El-Barbary, M.I. Heggie, Y.E. Lozovik, Phys. Rev. B 71 (2005) 113403.
[20] J.L. Rivera, C. McCabe, P.T. Cummings, Nanotechnology 16 (2005) 186.
[21] C.C. Ma, Y. Zhao, C.Y. Yam, G.H. Chen, Q. Jiang, Nanotechnology 16 (2005) 1253.
[22] E. Bichoutskaia, M.I. Heggie, A.M. Popov, Y.E. Lozovik, Phys. Rev. B 73 (2006) 045435.
[23] A. Kis, K. Jensen, S. Aloni, W. Mickelson, A. Zettl, Phys. Rev. Lett. 97 (2006) 025501.
[24] J. Servantie, P. Gaspard, Phys. Rev. B 73 (2006) 125428.
[25] B.T. Kelly, Physics of Graphite, Applied Science Publishers, London, 1981.
[26] F.M. Tong, C.Y. Wang, S. Ardhikari, J. Appl. Phys. 105 (2009) 094325.
[27] C.M. Wang, Y.Q. Ma, Y.Y. Zhang, K.K. Ang, J. Appl. Phys. 99 (2006) 114317.
[28] R. Chowdhury, C.Y. Wang, S. Adhikari, J. Phys. D: Appl. Phys. 43 (2010) 085405.
[29] C.Y. Wang, C.Q. Ru, A. Mioduchowski, J. Appl. Phys. 97 (2005) 024310.
[30] C.Y. Wang, L.C. Zhang, Nanotechnology 19 (2008) 195704.
[31] F. Scarpa, S. Adhikari, J. Phys. D: Appl. Phys. 41 (2008) 085306.
[32] F. Scarpa, S. Adhikari, C.Y. Wang, J. Phys. D: Appl. Phys. 42 (2009) 142002.